Thermal tracking of meltwater retention in Greenland's accumulation area

Neil F. Humphrey,[1] Joel T. Harper,[2] and W. Tad Pfeffer[3]

Received 9 May 2011; revised 20 October 2011; accepted 23 November 2011; published 25 January 2012.

[1] Poorly understood processes controlling retention of meltwater in snow and firn have important implications for Greenland Ice Sheet's mass balance and flow dynamics. Here we present results from a 3 year (2007–2009) field campaign studying firn thermal profiles and density structure along an 85 km transect of the percolation zone of west Greenland. We installed one or two thermistor strings at 14 study sites, each string having 32 sensors spaced between 0 and 10 m depth. Data from our network of over 500 sensors were collected at 15–60 min intervals for 1–2 years, thereby recording the thermal signature of meltwater infiltration and refreezing during annual melt cycles. We document three types of heating of firn related to different mechanisms of meltwater motion and freezing, including heterogeneous breakthrough events, wetting front advance, and year-round heating from freezing of residual deep pore water. Vertically infiltrating meltwater commonly penetrates through cold firn accumulated over decades, even where ice layers are present at the previous summer surface and where ice layer thickness exceeds several decimeters. The offset between the mean annual air temperature and the 10 m firn temperature reveals the elevation dependency of meltwater retention along our transect. The firn is > 10°C warmer than the mean annual air temperature at the region where meltwater runoff initiates. During 2007–2009, runoff was limited to elevations lower than ∼1500 m with no sharp "runoff limit"; rather, the ratio of retention to runoff transitioned from all retention to all runoff across a ∼20 km wide zone.

Citation: Humphrey, N. F., J. T. Harper, and W. T. Pfeffer (2012), Thermal tracking of meltwater retention in Greenland's accumulation area, *J. Geophys. Res.*, *117*, F01010, doi:10.1029/2011JF002083.

1. Introduction

[2] Significant increases in intensity and areal extent of surface melt have been documented recently on the Greenland Ice Sheet [*Hanna et al.*, 2005; *Mote*, 2007; *Steffen et al.*, 2004]. Surface melt affects overall mass balance of the ice sheet [*Ettema et al.*, 2010, 2009; *Mernild et al.*, 2010], as well as basal hydrology and ice flow dynamics [*Parizek and Alley*, 2004; *Zwally et al.*, 2002]. Surface melt can be segregated into melt in the ablation zone or melt in the accumulation zone, each of which is governed by different processes and has different implications if melt rates change. Increased melt in the ablation zone is at least partially responsible for thinning of the ice sheet margins in recent decades [*Krabill et al.*, 1999, 2004] and has been related to observed changes in basal sliding speeds [*van de Wal et al.*, 2008; *Shepherd et al.*, 2009; *Sundal et al.*, 2011]. However, substantial increases in melt extent observed over the last three decades occur in Greenland's accumulation zone. The implications of this increased melt in previously dry snow are less clear, and motivate the work presented in this paper.

[3] The "percolation zone" is the lower elevation reach of accumulation area experiencing some degree of surface melt. The percolation zone is highly affected by increased surface melt, and has substantial area for contributing runoff. Owing to the low slope of the ice sheet, the breadth of the percolation zone in Greenland is 50 km or more. Generally snow less than 1 year old is melted, but occasionally relatively young firn is also melted at the lowest elevations. Melt occurs on few days at the highest elevations of the percolation zone. Here, the snow surface is wetted, and a small amount of meltwater may infiltrate a short distance vertically, refreeze, and form thin ice layers [*Brown et al.*, 2011; *Parry et al.*, 2007]. The region extending up-glacier from the ELA to the bottom of the percolation zone – the region termed the "soaked facies" by *Benson* [1962], "percolation zone B" by *Müller* [1962], and later the "wet snow zone" by *Paterson* [1981] – general becomes fully saturated with water during the summer melt season. Under conditions of saturation, water can pool and perhaps penetrate the underlying ice mass, or water can migrate horizontally and become "runoff." Intermediate to the upper and lower ends of the percolation zone, the fate of melt is uncertain as it infiltrates vertically into firn and/or migrates horizontally through firn.

[1]Department of Geology and Geophysics, University of Wyoming, Laramie, Wyoming, USA.
[2]Department of Geosciences, University of Montana, Missoula, Montana, USA.
[3]INSTAAR, University of Colorado at Boulder, Boulder, Colorado, USA.

0148-0227/12/2011JF002083

[4] Water produced by melting snow in the accumulation zone is not initially free to escape but must first satisfy local thermal and hydraulic constraints before being mobilized to move along hydraulic gradients in the snow [*Colbeck*, 1975; *Pfeffer and Humphrey*, 1996; *Pfeffer et al.*, 1991]. The simplest model of the evolution of water flow in initially subfreezing, permeable firn was described by *Colbeck* [1975]: he proposed that water infiltrates vertically in a laterally uniform wetting front separating cold, dry firn ahead of the front from wet firn at 0°C and at residual saturation (the water-filled fraction of pore space required to overcome capillary trapping of water, usually estimated to be no more than ~7% of pore volume [*Colbeck and Anderson*, 1982]) behind the front. The amount of water necessary to establish wetted conditions behind the front is thus given simply by the latent heat required to warm firn of a given initial temperature and density to the melting point, plus the water required to fill the firn pore space (corrected for new ice formed in warming the firn) to residual saturation. *Colbeck* [1975] assumed that the speed of wetting front advance is controlled entirely by the surface melt rate, but this is an oversimplification of the actual front propagation [*Pfeffer et al.*, 1990]. The principal weakness in the 1-D Colbeck-type model of wetting front migration is the absence of heterogeneous infiltration, which is known to be dominant in subfreezing firn [*Marsh and Woo*, 1984; *Parry et al.*, 2007; *Pfeffer and Humphrey*, 1996], but is difficult to model in any way that provides robust, useful large-scale constraints on meltwater retention. Hence, application of this theory to the Greenland percolation zone is problematic and does not provide a reliable means for assessing the fate of meltwater.

[5] Additional uncertainty regarding meltwater's fate in the percolation zone stems from the role of ice layers in routing water. After a heavy melt year, large ice layers may form at or near the surface. Once formed, these ice layers may grow vertically and horizontally during the following melt season as new melt penetrates to depth and refreezes at the horizon of impermeable ice. After the cold content is satisfied by the release of latent heat, a "perched impermeable horizon" may develop, consisting of an ice layer or collection of ice layers forming a discrete barrier to vertical infiltration. Meltwater may then be conducted laterally along this surface with minimal vertical leakage to firn below. This scenario was postulated by *Müller* [1962] and developed by *Pfeffer et al.* [1991] as an end-member case for runoff, but such a structure has never been documented and, therefore, whether runoff can bypass underlying permeable firn by means of discrete impermeable barriers is unknown.

[6] Our understanding of the eventual fate of meltwater in most of the percolation zone thus remains poor owing to our lack of knowledge of heterogeneous infiltration and processes related to ice layers. At the highest elevations in the percolation zone, melt cannot satisfy runoff requirements and all surface melt is retained by pore-filling or ice layer growth. At the lowest elevations thermal and saturation requirements for runoff are easily met, and water is free to escape the ice sheet. But the fate of meltwater produced over much of the vast extent of the percolation zone between these clearly defined end-members is unclear. Perhaps the melt travels long horizontal distances along perched impermeable horizons, or perhaps it migrates vertically to fill pore space in the firn column; at present, no methods exist to track this water motion. Understanding the motion and ultimate fate of meltwater produced in the percolation zone of the Greenland Ice Sheet is critical to understanding the implications of the observed increases in surface melt. Neither changes in the mass balance nor the subglacial hydrology of the ice sheet can be inferred from knowledge of changes in surface melt alone; the routing of water, especially through the critical surface firn, must first be established.

[7] Here we address these issues through detailed field measurement of the thermal signature of meltwater infiltration and retention. We present a transect of thermal measurements across the percolation zone that document latent heating of the firn column caused by refreezing meltwater. We show that across much of the percolation zone, meltwater infiltrates deeply, well beyond the previous year's accumulation, to depths greater than 10 m. This infiltration bypasses thick ice layers. Lower in the percolation zone, meltwater slowly migrates horizontally through pore space deep in the firn column. We use our transect of measurements to delineate the percolation zone into regions where meltwater either (1) travels vertically and freezes or (2) travels horizontally and becomes free to escape.

2. Study Transect

[8] Our study was undertaken on the western flank of the Greenland Ice Sheet, north of the Illulissat (Jakobshaven) Ice Stream. Several other field investigations have reported on various aspects of this region [e.g., *Benson*, 1962; *Braithwaite et al.*, 1994; *Fischer et al.*, 1995; *Parry et al.*, 2007; *Pfeffer and Humphrey*, 1996]. We conducted our field research during the summers of 2007–2009 along a ~85 km transect (Figure 1) spanning most of the "percolation zone" as defined by *Benson* [1962]. Fifteen intensive study sites were spaced 5–10 km apart along our transect, and some additional observations were collected between these sites. The intensive study sites ranged from 1300 to 2000 m elevation. The mean slope is just under 1/2 degree, but some steeper ridges and valleys occur where the slope ranges from zero to a few degrees over a distance of about 1 km.

[9] Long-term automated weather stations, part of the AWS network of stations located on the ice sheet [*Steffen et al.*, 1996], exist at the upper end of the study transect (Crawford Point) and 25 km below the lower end of the traverse (Swiss Camp). A terrestrial station with a record extending to the late 1950s is located in Ilulissat, about 100 km from the bottom of our transect. We installed a temporary weather station of our own at site T1 for the duration of the project. Air temperatures at meteorological stations show that 2007 was an exceptionally warm year in western Greenland with record melt duration [*Box et al.*, 2008], while 2008 had a unusually cool winter and spring [*Box et al.*, 2009]. Temperatures in 2009 were intermediate, but our data do not extend past the cool spring conditions of May 2009.

[10] Although our transect experiences substantial summer melt, it lies entirely above the ELA located near Swiss Camp [*Box et al.*, 2006] and the surface remains snow covered throughout the melt season. Typical winter snow accumulation is on the order of 0.5 m water equivalent [*McConnell et al.*, 2000; *Bales et al.*, 2001; *Burgess et al.*,

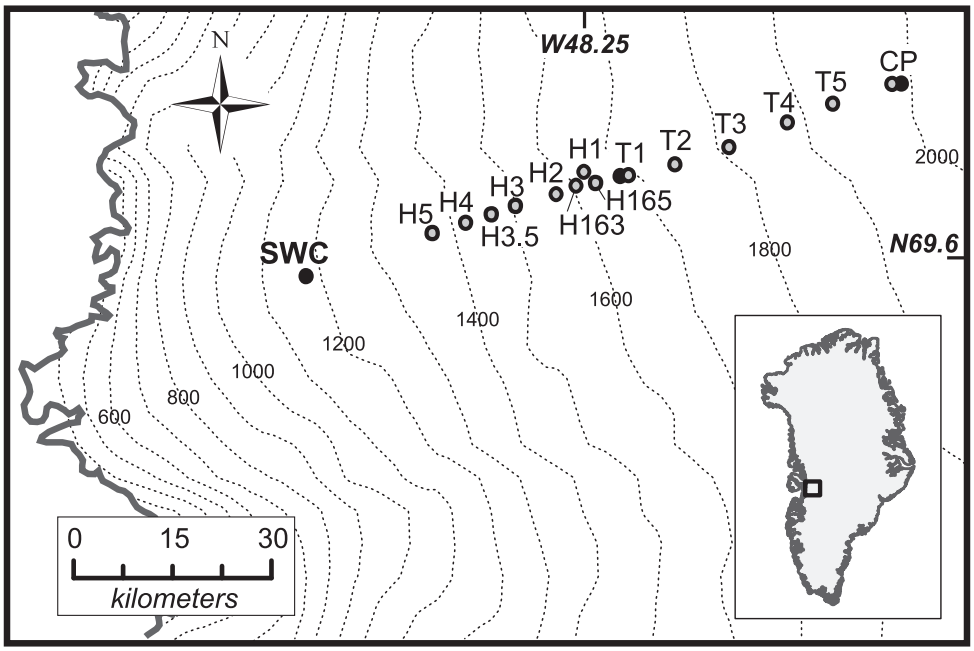

Figure 1. Map showing study transect and sites with thermistor string installations. Topography is from *Bamber et al.* [2001], shown with 100 m contours as dashed lines. Sites with thermistor strings are shown by gray dots. Sites with meteorological stations are shown by black dots. Contours of digital elevation model are approximate and do not exactly match known elevations of specific sites. SWC, Swiss Camp; CP, Crawford Point.

2010]. *Box et al.* [2004] show that over the span of our transect the accumulation varies by only about 0.04 m water equivalent (~8%). Assuming an initial snow density of 0.375 kg/m^3 [*Braithwaite et al.*, 1994] implies that a meter or more of snow depth accumulates along the transect each year. This fits well with observations during our 3 year study period. The average number of melt days observed by satellite radar backscatter ranges from 13 at Crawford Point to 70 at Swiss Camp, although there is strong interannual variability with Crawford Point having some years with near-zero melt days and other years with close to 30 [*Abdalati and Steffen*, 2001]. The surface mass balance therefore varies greatly over the length of our transect owing to the strong elevation gradient in melt, but not in accumulation.

3. Data Collection

[11] We measured high time resolution thermal profiles in the upper 10 m of the firn column by installing temperature sensors in core holes drilled at each of our 14 intensive study sites (Figure 1). The cores were drilled using a 9 cm diameter Kovacs drill with a gasoline powered drive. At each site, 2–9 cores extending to at least 10 m depth were extracted and logged for physical stratigraphy and density. Detailed core observations will be reported elsewhere. One core hole was selected at each site for instrumentation with a 32 sensor thermistor string. The lowest thermistor of the strings was installed at a depth of 10 m below the current snow surface. The core holes were then backfilled with fine-grained cold snow. A site located midway along our transect (T1) included two thermistor strings for comparison, making the total number of full depth sensor installations 15 (Table 1). In addition, two shorter 3 m strings were installed at sites H1 and H3.5 for comparison and for detailed analysis of the near-surface snow regime.

[12] The thermistor strings consisted of 32 thermistors spliced into a 38 conductor cable and mounted on the outside of the cable jacket. The spacing between sensors was 0.25 m from 0 to 5.25 m depth, and then 0.5 m to 10 m depth. Sealed 50K ohm thermistors were used to reduce the potential of self heating. The thermistors have a nominal 1% accuracy, and performance of a sampled subset was checked from +5°C to −15°C and compared to manufacturer supplied thermistor calibration curves. All thermistors were given a one-point calibration both in a cold room and in the field with a snow/water bath prior to emplacement. As a result of our calibrations we believe that the temperatures measured are accurate to better than 0.25°C. The data were recorded to a precision of 0.02°C. Aging of the thermistors over this multiyear study caused some thermistors to drift by up to 0.25°C. Hence, we believe that combined errors make our temperature measurements accurate to about 0.5°C or better.

[13] Data were continuously recorded on 32-channel, 12 bit data loggers. The data loggers were fixed to the top of the thermistor strings and mounted on a pole extending above the snow surface. Data were stored in flash, nonvolatile, memory. The loggers operated for the duration of the project, recording measurements every 10–20 min in summer and every 60 min during winter, using Greenland local time (UTC −3 h) and Julian days. Water condensation within the logger cases in 2007 caused some data loss during the winter of 2007–2008. We solved the problem in 2008 and subsequently had complete data recovery.

[14] The installation and downloading of the thermistor strings was staggered and therefore data do not cover

Table 1. Location and Records of Thermistor Strings

Site	Latitude (deg)	Longitude (deg)	Elevation	Date Installed	Date Downloaded
Crawford Point	69.87650	47.01020	1997	27 May 2007	27 May 2008
T5	69.84802	47.27358	1932	27 May 2007	29 May 2007
T4	69.81998	47.45050	1877	1 June 2007	27 May 2008
T3	69.78360	47.67018	1819	27 May 2007	27 May 2008
T2	69.75693	47.88028	1750	30 May 2007	27 May 2008
T1–07	69.73802	48.06097	1710	30 May 2007	16 May 2009
T1–08	69.73802	48.06097	1710	24 May 2008	16 May 2009
H163	69.72505	48.19020	1680	29 May 2008	15 May 2009
H1	69.73908	48.24030	1660	17 May 2008	15 May 2009
H165	69.71978	48.26740	1644	22 May 2008	15 May 2009
H2	69.70617	48.34497	1555	18 May 2008	15 May 2009
H3	69.68743	48.49967	1540	19 May 2008	18 May 2009
H3.5	69.67393	48.59112	1497	21 May 2008	15 May 2009
H4	69.66018	48.68945	1401	23 May 2008	15 May 2009
H5	69.64372	48.81594	1370	13 May 2009	15 May 2009

identical time intervals at all sites along the transect (Table 1). The five upper holes were installed in 2007. These sites were downloaded in 2008, but snow accumulation in 2009 buried the data loggers at the highest three sites (CP, T4, T3), so records from only T1 and T2 were retrieved in 2009. The lower six sites were installed in 2008, and collected data over summer-winter 2008–2009. A final hole was installed below the lowest site in 2009 (H5), but was only logged for 2 days during 2009. We installed two temperature strings located 10 m apart at site T1, one in 2007 and one in 2008; these allow comparison of data obtained at slightly different locations of the same site, using different thermistor strings and data loggers.

[15] For comparison to our field data, we employ a thermal model for firn based on conductive heat transfer only. Our model uses a 1-D implicit transient finite difference scheme to solve the diffusion equation. We assume constant density, based on field measured site averages, and thermal conductivities based on an average of the *Van Dusen* [1929] and *Schwerdtfeger* [1963] equations. Insufficient meteorological data are available for employing a full energy balance at the surface. We therefore parameterize the surface boundary condition on the basis of temperature and net solar radiation observations from nearby stations. We installed a temporary weather station at site T1, and permanent "GC-Net" stations are located at Crawford Point and Swiss Camp [*Steffen et al.*, 1996] but were not always operational during our study. Fortunately, at least one GC-Net station was working at any given time, which we used with our station to construct cross-correlated records. A single multiplicative correction factor is introduced to the upper 0.25 m conductivity, and is calibrated to winter (below freezing) thermal conduction of surface air temperature into the firn column. Solar radiation heating consists of a correction factor times the net solar and is also calibrated to the winter period.

4. Results

4.1. Measurement Integrity

[16] A short-lived thermal disturbance of the firn column was caused by the core hole drilling, the installation of the thermistor cable, and the backfilling processes. The temperatures at 10 m depth always stabilized to within a fraction of a degree of their final values in less than a day after emplacement. This is not unexpected considering the low heating from mechanical drilling together with the relatively low heat capacity and high thermal conductivity of firn compared to glacier ice, which is known to have a recovery time on a scale of days [*Humphrey*, 1991]. Once recovered, the two thermistor strings installed 10 m apart at site T1 exhibited temperature profiles which did not differ by more than their 0.5°C accuracy (Figure 2), implying repeatability of measurements at the "site" scale. Exceptions to this agreement occurred during transient heating anomalies, which are discussed in section 4.2.1.

[17] The black thermistor cables were susceptible to solar heating near the surface. In addition, the copper thermistor cable, although small gauge (0.4 mm), conducts heat well. The net thermal conductivity of the wire bundle is comparable to a column of ice 3 cm in diameter. This implies that some heat can be conducted up and down the wires and we expect smoothing and degradation of the temperature signal at the 5–10 cm scale. We sometimes observed anomalously

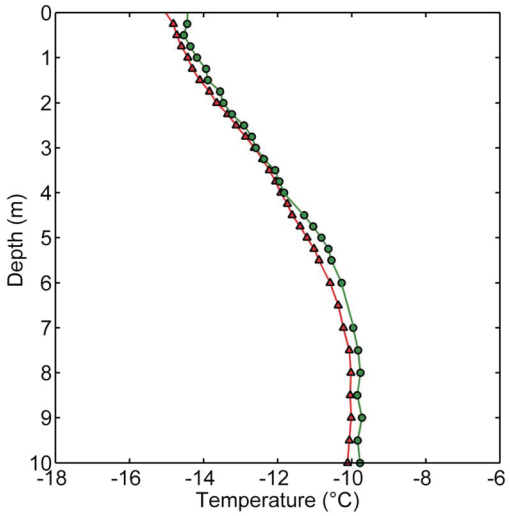

Figure 2. Temperature profile repeatability. Data are from two thermistor strings installed 10 m apart at site T1 and show a snapshot of temperatures on 5 May 2009. The two records agree within 0.5°C of each other. However, transient heating events due to localized meltwater infiltration and refreezing created marked differences between the two temperature profiles for periods of days to weeks.

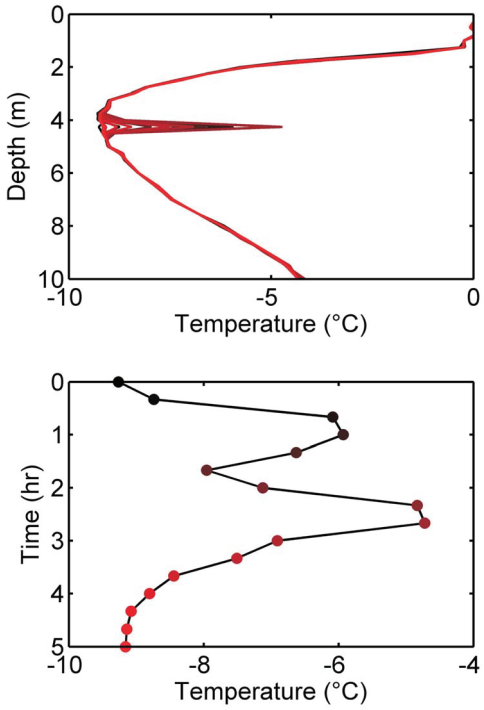

Figure 3. Transient freezing events beginning at 11:00 h on day 170 (18 June 2008): (top) thermistor readings at all depths and (bottom) time series of the thermistor at 4.25 m depth, with time starting at 11:00 h. Shown are two events which occurred in close succession at the same depth, implying two waves of infiltrating/refreezing meltwater. Time step between temperature profiles is 20 min. Maximum heating was 3.3°C during the first event and 4.4°C during the second. The first event cooled for less than an hour, before heating from the second event. The composite heat anomaly decayed to background levels after about 2–3 h.

warm readings in the upper 50 cm that became exposed to air and sun in a narrow melted-out ring of adjacent snow. We therefore consider readings above 1 m depth to be suspect.

[18] A major concern with our installation method is the potential for meltwater to move down the path of the borehole which cuts the natural stratigraphy, but in this largely unsaturated flow regime, a backfilled borehole is likely a flow barrier [*Pfeffer and Humphrey*, 1998] not a flow pathway. More concretely, our data indicate such flow did not occur. Water motion down the boreholes would lead to progressive warming along a length of borehole, and this is not observed in our data. Indeed our data are dominated by spatially confined refreezing events that rarely reach 0°C, indicating refreezing occurring at some horizontal distance from the borehole and not by water traveling down the borehole.

4.2. Refreezing Processes

4.2.1. Transient Breakthrough Events

[19] We commonly observed heating events consisting of strong temperature deviations away from stabilized temperature profiles. These events lasted hours to days, they affected limited 0.25 to 1.5 m reaches of the profiles, and were observed at all depths along our thermistor strings (Figure 3). The short-lived warming anomalies could only be due to the release of latent heat from refreezing meltwater; no other sensible heat source exists at depth. The magnitude of warming caused by latent heating events is revealed by comparison of measured profiles with modeled profiles based on conductive heat transfer only. For example, Figure 4 shows a substantial freezing event at site H2 recorded by at least six different thermistors over a 1.5 m reach and causing up to 5°C of local warming. This event must have occurred away from the thermistor string since the temperatures are not fully warmed to 0°C. The combination of multiple events over time in the upper 5 m of the firn column warmed the entire profile by up to 10°C from a hypothetical profile based on the model of only conductive heat transfer.

[20] The transient nature and spatially limited extent of latent heating events indicates heterogeneous infiltration with refreezing along vertical "pipes" [*Marsh and Woo*, 1984; *Pfeffer and Humphrey*, 1998]. Simple dye tracing experiments and pit excavations in the upper few meters of snow and firn provide visual confirmation of vertical meltwater infiltration along pipes (Figure 5). Impeded by an ice layer or grain-size transition, water accumulates until residual saturation is reached. Eventually a breakthrough event occurs along the vertical pipe. The piping process is spatially and temporally discontinuous and leads to significant lateral inhomogeneity of the ice structure in the firn column. The heterogeneous features are enhanced by subsequent piping and ice layer/lens formation.

[21] Although we observe thick ice layers of decimeter-to-meter thickness, they are notably discontinuous in radar profiles [*Brown et al.*, 2011]. Our thermal measurements document water bypassing ice layers formed at the previous summer surface, as well as deeper ice layers decimeters or more in thickness. For example, Figure 6 illustrates

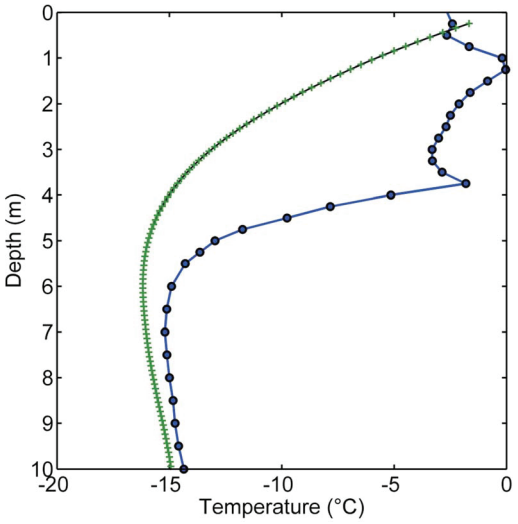

Figure 4. Infiltration heating event at site T3 occurring at midnight on day 204, 2007 (late July). Dots mark the measured temperature profile, with heating events at about 1.5 and 4 m depth. Crosses show the conductively modeled temperature profile based on measured air temperatures as the surface boundary condition.

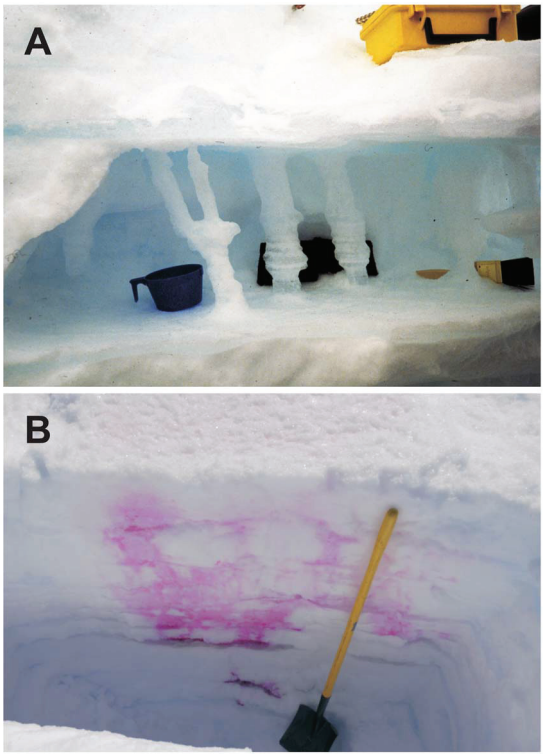

Figure 5. Photographs showing evidence of heterogeneous meltwater infiltration: (a) photograph showing excavated ice pipes and (b) photograph showing infiltration pathways and ice lenses accentuated by red dye in a ~1.5 m deep snow pit at Crawford Point. Note isolated ice lens at bottom of pit.

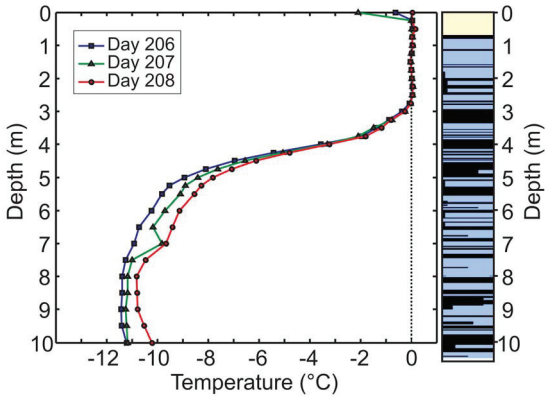

Figure 6. Deep infiltration heating event: (left) temperature profiles and (right) corresponding firn and ice stratigraphy. Three temperature profiles at site T1 at 04:00 h on three successive days during late July 2007 are shown. The snow and firn are isothermal at the melting point from the surface to a depth of 3 m. A relatively minor transient warming event occurs on day 207 at 7 m depth. Temperature at 10 m depth warms by 1°C from day 207 to day 208, which along with the downward warming temperature gradient on day 208 implies that water infiltrates to depths greater than 10 m. Stratigraphy is categorized into new snow (tan), firn (blue), and ice (black). Black coloring of the stratigraphic column indicates fraction of core occupied by ice layers, lenses, or pipes (black coloring crossing the whole column indicates 100% of core diameters occupied by ice; black coloring crossing half of the column indicates 50% of the core occupied by ice, etc.).

stratigraphy and temperature profiles at site T1, midway along our transect at 1710 m elevation. An ice layer 0.1 m thick exists at the previous year's summer surface at 0.70–0.80 m depth. Eight thinner ice layers and other ice pipes are present in the upper 3 m of the core, and then a massive ice layer 0.42 m thick extends from 2.94 to 3.36 m depth. The meltwater has bypassed both the 0.1 m thick ice layer formed at the previous summer melt surface, and the thick ice layer below 2.94 m depth. Hence, while ice is essentially impermeable, our data shows that even thick ice layers in firn are not vertical flow barriers.

4.2.2. Surface Wetting Fronts

[22] We observed that repeated piping events sometimes warmed the firn ahead of a slowly advancing wetting front (Figure 7). This is indicated by our time series of temperature profiles that document downward penetration of breakthrough heating events, followed by slow progression of the wetting front where the snow and firn become a uniform 0°C. Hence, heterogeneous breakthrough events and an advancing wetting front appear to be intimately related, with wetting front advance following a number of piping events (Figure 8). Eventually the melt simply moves homogeneously from the surface through the snow and firn, instead of along discrete pipes. We only observed wetting front advances accompanied by heterogeneous piping ahead of the front, but we did observe heterogeneous wetting without a clearly defined wetting front. This implies that the heterogeneous wetting is a necessary but not sufficient condition for a wetting front to develop. The entire process is

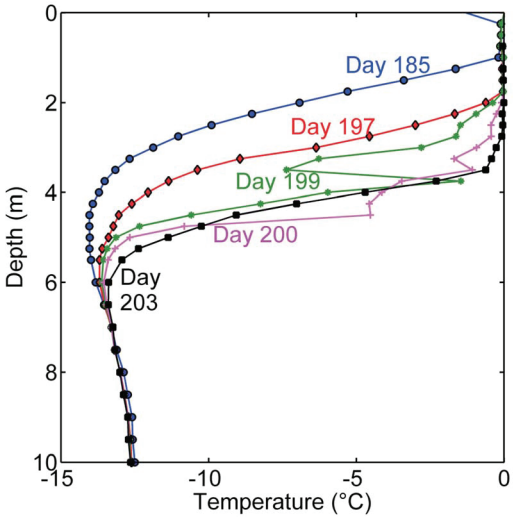

Figure 7. Five time slices of temperature versus depth during the summer of 2007 at site T2 showing wetting front migration. On day 185 (5 July) the upper 1 m of the firn column was wetted and at 0°C. Slow downward motion of the wetting front moved the 0°C isotherm to more than 2 m depth by day 197. Significant piping events at depths > 4.5 m on days 197 and 199 are shown. These events warmed firn below the maximum depth of the wetting front. The wetting front halted downward progress at 3.75 m depth on day 200 (July 22).

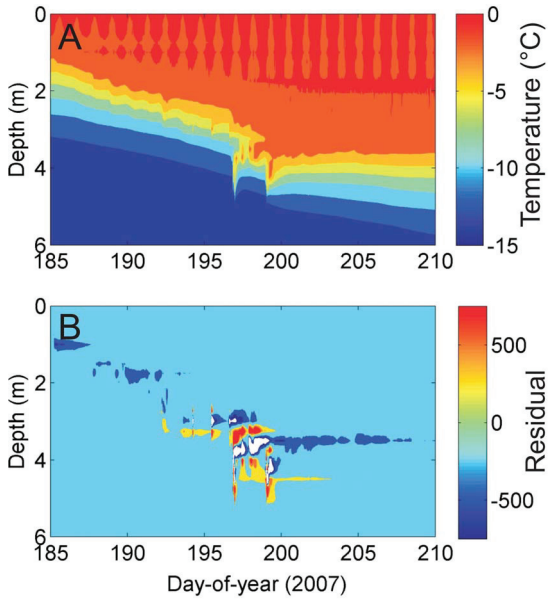

Figure 8. Time versus depth detail for the upper 6 m, at the same site and time interval as that in Figure 7. (a) Color contour interval of 2.5°C. Strong diurnal heating/cooling events occur in the upper 1–2 m. The isotherms show steady progression into the firn column (days 185–195), with punctuated infiltration events (i.e., days 195–200). (b) Locations of refreezing and heterogeneous water flow. Differences (or residual) between observed rate of temperature change as well as the curvature of the temperature profile are plotted. Zero residual is expected for pure heat conduction; however, residuals occur where temperature is changing faster (positive) or slower (negative) than conduction heat transfer. Residuals have multiple sources, but three of the largest are generated by refreezing. Refreezing at a wetting front creates long-term negative residuals, refreezing of a transient ice lens creates large but short-lived spikes of both polarity, and most interestingly, heterogeneous (away from the borehole) refreezing collapses into only positive residuals, after an initial spike. Units are in rates of temperature change per day; however, since we are differentiating noisy data, the scale should be considered qualitative.

complicated by cold-clear nights, where substantial heat can be lost to the atmosphere [*Rick et al.*, 2008]. On consecutive cold days the wetting front can freeze in place and the 0°C isotherm rises partly back up the profile. Further, our sensors showed an obvious and extensive wetting front during the heavy melt year of 2007, but show minimal evidence of a wetting front during the colder summer of 2008 despite extensive piping events. While our data are sufficient to confidently reveal these processes, the finer details are elusive owing to the suspect nature of selected measurements near the surface as discussed in section 4.1.

4.2.3. Deep Pore Space

[23] In addition to heterogeneous heating and wetting front-type heating, we observed deeply sourced heating at rates that remained steady over time scales of months. This type of heating is distinctly different from the transient events associated with piping, and did not occur at all locations: we only observed this at sites below T1. The thermal gradients in successive temperature profiles indicate heat originating below the bottom of the thermistor strings, deeper than 10 m. For example, the thermistor string at site H2 documented slow steady heating for more than half of a year, continuing throughout an entire winter (Figure 9). Such a thermal signal could only be caused by slow refreezing of a mass of water located at depths greater than 10 m. The water begins freezing in early winter and continues to freeze through the following spring. The duration and thermal gradients of this warming implies that tens of centimeters of water were frozen in order to supply the required heat energy. The origin of this water is probably not local to the site, since heating started after the onset of winter; therefore this observation implies some amount of lateral water motion at depth.

4.3. Temperature at 10 m Depth

[24] Year-to-year changes in the temperature at 10 m depth were relatively small, although interannual comparisons are complicated by the fact that only a subset of the sites were measured in any given year. The difference between 2007 and 2008 temperatures grow with decreasing elevation between Crawford Point and T1, from 0.45°C at Crawford Point to 1.25°C at site T1. Temperatures in 2008 were always warmer. The largest observed change from year to year occurred at site H2, with a 2.6°C difference between 2008 and 2009. Sites lower than this show far less annual variability, with site H4 demonstrating less than a 0.1°C change from 2008 to 2009.

[25] The temperatures at 10 m depth at each of the sites demonstrate strong gradients along the length of the study

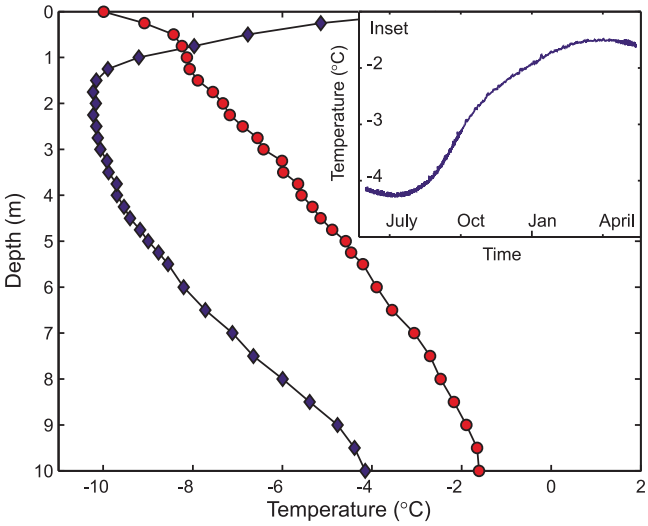

Figure 9. Two temperature profiles at site H2: 30 May 2008 (diamonds) and 15 May 2009 (dots). Both profiles show an upward cooling temperature gradient between about 1.5 and 10 m depth. Warm spring temperatures in late May of 2008 have heated the upper meter of the profile, but no such spring warming has yet occurred in 2009. The 10 m temperature has warmed by more than 2°C between the two profiles, demonstrating a deeper heat source. Inset shows the progressive heating of the firn at 10 m depth spanning the year between the profiles, while surface air temperatures remained cold during winter.

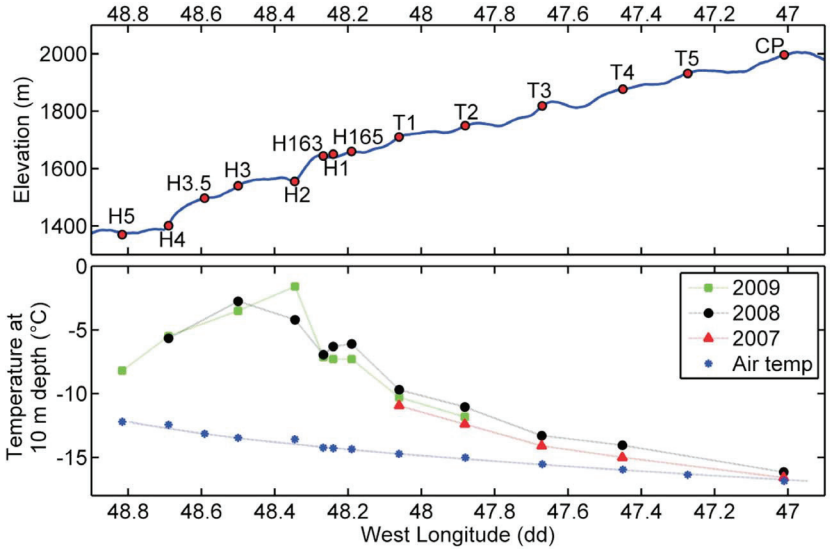

Figure 10. Comparison of deep firn temperature with air temperature along 85 km study transect. (top) Elevation profile along study transect measured by a 2009 NASA Airborne Topographic Mapping flight [*Krabill et al.*, 2002]. Vertical exaggeration is more than 100 times. Red dots show locations of thermistor strings. (bottom) Temperature at 10 m depth at 12 study sites, with different years indicated by color. Blue asterisks show mean annual air temperature computed for the specific elevation of each study site.

transect (Figure 10). As elevation decreases below 2000 m, the temperatures increase steadily to a maximum at ~1500 m elevation. The warming gradient along this reach averages about +3.75°C per 100 m of elevation loss. However, the warming gradient is not linear: most warming occurs between sites T2-H2, 1800 and 1550 m elevation. The maximum 10 m temperature is about 15°C warmer than at 2000 m elevation and is only a few degrees below the melting point. After this maximum at ~1500 m elevation, the 10 m temperatures begin cooling with decreasing elevation. The temperatures cool along a relatively linear gradient at a rate of about −2.8°C per 100 m of elevation loss. By site H5 at 1350 m elevation, the temperatures have cooled by about 7°C from the warmest temperature at higher elevation.

[26] The trends in measured 10 m temperatures can be contrasted with the mean annual air temperature, predicted to decrease with elevation following the linear lapse rate we employ (Figure 10). Firn temperature at 10 m depth closely approximates the mean annual air temperature at Crawford Point (2000 m elevation), while the deep firn warms with decreasing elevation to ~1500 m, diverging from the mean annual air temperature, which warms much less with decreasing elevation. Below ~1500 m the 10 m firn temperature cools as it increasingly converges with the colder mean annual air temperature at the surface.

5. Discussion

5.1. Infiltration and Retention

[27] We are not the first to document the existence of heterogeneous meltwater infiltration with piping to depths below the previous summer surface. For example, *Benson* [1962], *Müller* [1976], and *Braithwaite et al.* [1994] all note isolated freezing events associated with piping to several meters depth in Greenland or the Canadian Arctic. Our time-lapse measurements of bulk heating of the firn column from infiltration/refreezing events, however, allows us to document meltwater retention along the length of the percolation zone. And, our unique observations of freezing of pore water at depth within the firn column have important implications for runoff processes. Together these observations have implications for delineation of the runoff limit.

[28] The amplitude of annual temperature variation falls to a small fraction of the surface amplitude at 10 to 15 m depth, for thermal diffusivity ranging from 16 $m^2\ yr^{-1}$ (typical for snow) to 37.2 $m^2\ yr^{-1}$ (for glacier ice). Thus, in the absence of other, nonconductive, modes of heat transfer, the temperature at 10 m depth can be expected to be very close to the mean annual surface air temperature [*Cuffey and Paterson*, 2010]. If the 10 m temperatures along our study transect (Figure 10) were dictated by purely conductive processes, we would expect our elevation transect of 10 m firn temperatures to closely match the lapse rate of the mean annual air temperature. Significant deviations from the lapse rate can only be caused by latent heating during meltwater freezing (other modes of transient heating, including frictional advective heating [e.g., *Clarke and Waddington*, 1991] are insignificant or absent at 10 m depths). Our detailed data on the firn column's temperature structure reveals the details of meltwater refreezing, while our transect of 10 m temperatures gives an integrated view of the timing and location of refreezing of meltwater, and thus contains information about meltwater migration over time and space.

[29] By the end of the winter cold season, during which time the surface snow and firn cools to well below 0°C, conductive heat transfer upward to the atmosphere has smoothed our thermal profiles. However, if substantial quantities of latent heat were added during the prior summer, the temperature profile below the upper few meters may still contain remnant heat, although conductive heat diffusion will have smoothed local anomalies. Thermal conduction in

Figure 11. Photograph showing surface feature interpreted to be similar to a pingo formed in permafrost regions.

firn will dissipate a temperature anomaly at 10 m depth at the rate of about 50% per year, so thermal anomalies at depth take longer than 1 year to fully dissipate. Consequently, our 10 m temperatures primarily represent the thermal balance between the previous winter and the previous melt season, although in cases where substantial latent heat has been added they may also contain attenuated information from seasons two or more years previously. For example, the slightly warmer 10 m temperatures we observed in 2008 likely reflect the heavy melt during the unusually warm 2007 melt season.

[30] We interpret the mismatch between the 10 m firn temperatures and the interpolated mean annual air temperature (Figure 10) as follows. At Crawford Point the 10 m temperature is essentially due to conductive heat transfer alone, and is thus roughly equivalent to the mean annual air temperature. As elevation decreases from Crawford Point, the steady warming of the 10 m firn temperature relative to the atmosphere indicates progressively more meltwater refreezing as the flux and penetration depth of surface melt infiltration increases. The temperature mismatch between firn and atmosphere intensifies as warming of the firn from latent heat, arising from advective heat transfer from penetrating meltwater, becomes progressively more important than conductive heat transfer to the atmosphere. This effect reaches a maximum in the region of sites H2-H3, 1550–1500 m elevation. At lower elevations, declining 10 m temperatures indicate less advective heating owing to decreasing quantities of infiltrating meltwater. This may seem counterintuitive given progressively higher rates of surface melt at lower elevation, but prior infiltration and refreezing events will have decreased firn water permeability. We know that at lower-elevation sites the melt is not trapped at shallow depths and does not refreeze there, since the full vertical temperature profiles at these sites remain below freezing and are not significantly different than at higher elevation sites. Hence, with descending elevation less and less melt penetrates and refreezes at depth. The "missing heat" at lower sites indicates missing water, or more importantly, indicates that water is moving horizontally as runoff.

[31] Our above interpretation of the transect of 10 m temperatures is based on a snapshot of conditions during the 2007–2009 period. Nevertheless, the average 10 m temperatures changed relatively little from year to year during our study despite anomalously warm and cold years. Hence, our snapshot appears representative of a multiyear time scale, but our interpretation rests upon having an entire transect of temperature profiles. Our refreezing versus runoff results can be summarized as follows. The region of the traverse where 10 m temperatures increase with decreasing elevation (Figure 10) is the region where melt is locally refrozen. The region where the 10 m temperatures decrease with elevation is the upper limit of the runoff zone. The central region (H2, H3) is the complex region of the runoff limit, with mixed refreezing and horizontal flow, with the details depending on yearly melt and subtle local spatial variations.

5.2. Deep Pore Water

[32] Our observations of heat originating from below 10 m depth (Figure 9) during the winter of 2008 suggest that lateral migration of a large mass of deep pore water is possible in some circumstances. Air temperature and surface firn temperature observations indicate minor melt in 2008 compared to the summer of 2007. The latter was a record-high melt year in western Greenland [e.g., *Tedesco*, 2007; *Box et al.*, 2008]. Therefore, the water mass filling deep pore space in the firn was likely generated during the summer melt season of 2007, but did not migrate to the site until many months later. This suggests that during the summer melt period, some areas at depth become fully saturated, and this meltwater slowly migrates down glacier under low hydraulic gradients. The pore water can persist for at least many months, until either escaping the system or refreezing. This may seem odd, given the mean temperature in this region is well below freezing, however the warmed firn effectively acts as thermal insulation for any pooled water. As an illustration, we calculate that a layer of water 20 cm thick between infinitely thick ice layers at -3°C, will take $\sim$2 years to completely refreeze. Thus, water can remain unfrozen beneath cold firn for extended periods. Thus, the conditions for water flow do not need to be satisfied at the surface in order to have migrating water at a particular coordinate of the ice sheet.

[33] Since the slope of the ice sheet in this region is low (less than 0.5°), the hydraulic gradient driving horizontal water flow is small, and very slow flow would be expected. Perhaps the water migrates by processes akin to smaller-scale piping, whereby massive ice is formed adjacent to sections of warmed permeable firn. Such flow would be highly heterogeneous in both time and space. Trapped water undergoing freezing sometimes appears to erupt to the surface, forming pingo-like ice masses similar to those found in permafrost regions (Figure 11). These features consist of refrozen saturated snow, standing up to 3 m above the mean surface with horizontal dimensions of 10s of meters, and often form at slight changes in slope from steep to shallow. We identified these features in the limited elevation band between H2 and H4, and only in 2008 following the heavy melt year of 2007. We expect that rare circumstances of

confining pressure are required to form these pingos and that they would not exist above all areas of saturated firn. Since we did observe at least five within 1 km of our transect, we postulate that that deeply water saturated firn conditions were in fact common.

5.3. Partitioning Runoff

[34] Our data imply that substantial quantities of water penetrate deeply via heterogeneous breakthrough processes, creating fully saturated firn at depth. We cannot place a maximum constraint on the depth of penetration, but we show that it commonly exceeds 10 m. *Benson* [1962] also noted that isolated deep flow fingering events occur, but his shallower and less dense measurements apparently failed to identify the relevance of this in percolation zone processes and structure. The ability of surface melt to penetrate through multiple years of accumulation has strong implications for the definition of the runoff limit: it cannot be a simple dividing line separating areas with runoff from areas with no runoff; nor can it be easily delineated by an examination (or modeling) of the previous year's accumulation and melt conditions. Rather, we suggest that runoff initiation occurs over a zone extending 10s of km in length along the percolation zone. At the upper limit of this zone, all surface melt refreezes locally, and at the lower limit, the entirety of a season's melt escapes; in between, a variable fraction of a season's melt is consumed by creating conditions that mobilize flow. Since water penetrates deeply within the intermediate zone, and migrates slowly through pore space, there can be no such thing as a single-year, linearly distinct runoff limit.

6. Conclusions

[35] Surface melt of Greenland's accumulation area fingers vertically into underlying cold snow and firn. Infiltrating meltwater can bypass impermeable ice layers formed at the previous summer surface and massive ice layers formed at depth. Meltwater penetrates through multiple years of accumulation to depths of 10 m or more, without warming the bulk firn to the melting point. In places, water occupying pore space at depths below 10 m migrates slowly along low hydraulic gradients for periods of many months to perhaps a year or more. Infiltrating and freezing meltwater heats the firn in the percolation zone, although the bulk of the firn remains below freezing. Our temperature time-lapse measurements spanning the percolation zone document firn heating related to different mechanisms of meltwater migration: (1) transient meltwater breakthrough events, (2) advance of a uniform wetting front, and (3) deep migrating pore water. The first occurs at all elevations of the percolation zone, the second is only substantial during heavy melt years, and the last is limited to the lower elevations where horizontal water flow occurs.

[36] The mismatch between the temperature at 10 m depth in firn and the mean annual surface temperature yields a measure of melt retention by refreezing: at elevations where retention is minimal the 10 m firn temperature is dominated by conductive heat flow and approximates the mean annual surface temperature; where advected latent heat has been added to the firn by retention, the 10 m firn temperature is substantially warmer than the mean annual surface temperature. During the 3 year interval of our study we conclude that between 2000 m and ~1500 m elevation, all surface melt is retained in the firn column. Below ~1500 m elevation, water begins to move horizontally with fractions retained and fractions potentially running off. Water can persist and migrate at depth despite cold conditions in the firn. Therefore migrating meltwater cannot be strictly identified on the basis of near-surface conditions. Runoff occurs while the bulk of the firn is below freezing. Furthermore, the runoff limit is a zone, not a distinct line, where an increasing fraction of meltwater becomes mobilized for horizontal transport. By 1350 m all melt is available for runoff once the conditions for runoff have been satisfied in the previous winter snowfall.

[37] The processes that dictate runoff occupy at least the upper 10 m of the snow/firn column, and therefore would be difficult to remotely sense. Our thermal measurements have increased the understanding of these processes, and our methods provide a robust technique for ground truthing, without actually observing runoff. However, our ground-based approach is time and labor consuming, and is ill suited for extension to the entirety of the lower accumulation zone of the Greenland Ice Sheet. A remaining challenge is to investigate whether a remotely accessible variable (perhaps a meteorological parameterization, or possibly a surface morphological variable) can delineate the runoff transition zone. With such delineation around the perimeter of ice sheet, climatically forced surface mass balance modeling of the ice sheet can proceed with substantially greater confidence.

References

Abdalati, W., and K. Steffen (2001), Greenland ice sheet melt extent: 1979–1999, *J. Geophys. Res.*, *106*, 33,983–33,988, doi:10.1029/2001JD900181.

Bales, R. C., J. R. McConnell, E. Mosley-Thompson, and B. Csatho (2001), Accumulation over the Greenland ice sheet from historical and recent records, *J. Geophys. Res.*, *106*, 33,813–33,825, doi:10.1029/2001JD900153.

Bamber, J. L., R. L. Layberry, and S. Gogineni (2001), A new ice thickness and bed data set for the Greenland ice sheet: 1. Measurement, data reduction, and errors, *J. Geophys. Res.*, *106*, 33,773–33,780, doi:10.1029/2001JD900054.

Benson, C. S. (1962), Stratigraphic studies in the snow and firn of the Greenland ice sheet, *Res. Rep. 70*, 120 pp., Snow, Ice and Permafrost Res. Estab., U. S. Army Corps of Eng., Hanover, N. H.

Box, J. E., D. H. Bromwich, and L. S. Bai (2004), Greenland ice sheet surface mass balance 1991–2000: Application of Polar MM5 mesoscale model and in situ data, *J. Geophys. Res.*, *109*, D16105, doi:10.1029/2003JD004451.

Box, J. E., D. H. Bromwich, B. A. Veenhuis, L. S. Bai, J. C. Stroeve, J. C. Rogers, K. Steffen, T. Haran, and S. H. Wang (2006), Greenland ice sheet surface mass balance variability (1988–2004) from calibrated polar MM5 output, *J. Clim.*, *19*(12), 2783–2800, doi:10.1175/JCLI3738.1.

Box, J., J. Cappelen, D. Bromwich, L.-S. Bai, T. Mote, B. Veenhuis, N. Mikkelsen, and A. Weidick (2008), Greenland, in *State of the Climate in 2007*, edited by D. H. Levinson and J. H. Lawrimore, *Bull. Am. Meteorol. Soc.*, *89*, S94–S97.

Box, J. E., et al. (2009), Greenland, in *State of the Climate in 2008*, edited by T. C. Peterson and M. O. Baringer, *Bull. Am. Meteorol. Soc.*, *90*, S108–S112.

Braithwaite, R. J., M. Laternser, and W. T. Pfeffer (1994), Variations of near-surface firn density in the lower accumulation area of the Greenland Ice-Sheet, Pakitsoq, West Greenland, *J. Glaciol.*, *40*(136), 477–485.

Brown, J., J. Harper, W. T. Pfeffer, N. F. Humphrey, and J. Bradford (2011), High-resolution study of layering within the percolation and soaked facies of the Greenland Ice Sheet, *Ann. Glaciol.*, *52*(59), 35–42.

Burgess, E. W., R. R. Forster, J. E. Box, E. Mosley-Thompson, D. H. Bromwich, R. C. Bales, and L. C. Smith (2010), A spatially calibrated model of annual accumulation rate on the Greenland Ice Sheet (1958–2007), *J. Geophys. Res.*, *115*, F02004, doi:10.1029/2009JF001293.

Clarke, G. K. C., and E. D. Waddington (1991), A 3-dimensional theory of wind pumping, *J. Glaciol.*, *37*(125), 89–96.

Colbeck, S. C. (1975), Theory for water-flow through a layered snowpack, *Water Resour. Res.*, *11*, 261–266, doi:10.1029/WR011i002p00261.

Colbeck, S. C., and E. A. Anderson (1982), The permeability of a melting snow cover, *Water Resour. Res.*, *18*, 904–908, doi:10.1029/WR018i004p00904.

Cuffey, K. M. S., and W. S. B. Paterson (2010), *The Physics of Glaciers*, 4th ed., 693 pp., Elsevier, Amsterdam.

Ettema, J., M. R. van den Broeke, E. van Meijgaard, W. J. van de Berg, J. L. Bamber, J. E. Box, and R. C. Bales (2009), Higher surface mass balance of the Greenland ice sheet revealed by high-resolution climate modeling, *Geophys. Res. Lett.*, *36*, L12501, doi:10.1029/2009GL038110.

Ettema, J., M. R. van den Broeke, E. van Meijgaard, and W. J. van de Berg (2010), Climate of the Greenland ice sheet using a high-resolution climate model–Part 2: Near-surface climate and energy balance, *Cryosphere*, *4*(4), 529–544, doi:10.5194/tc-4-529-2010.

Fischer, H., D. Wagenbach, M. Laternser, and W. Haeberli (1995), Glacio-meteorological and isotopic studies along the EGIG line, central Greenland, *J. Glaciol.*, *41*(139), 515–527.

Hanna, E., P. Huybrechts, I. Janssens, J. Cappelen, K. Steffen, and A. Stephens (2005), Runoff and mass balance of the Greenland ice sheet: 1958–2003, *J. Geophys. Res.*, *110*, D13108, doi:10.1029/2004JD005641.

Humphrey, N. (1991), Estimating ice temperature from short records in thermally disturbed boreholes, *J. Glaciol.*, *37*(127), 414–419.

Krabill, W., E. Frederick, S. Manizade, C. Martin, J. Sonntag, R. Swift, R. Thomas, W. Wright, and J. Yungel (1999), Rapid thinning of parts of the southern Greenland Ice Sheet, *Science*, *283*(5407), 1522–1524, doi:10.1126/science.283.5407.1522.

Krabill, W. B., W. Abdalati, E. B. Frederick, S. S. Manizade, C. F. Martin, J. G. Sonntag, R. N. Swift, R. H. Thomas, and J. G. Yungel (2002), Aircraft laser altimetry measurement of elevation changes of the Greenland ice sheet: Technique and accuracy assessment, *J. Geodyn.*, *34*(3–4), 357–376, doi:10.1016/S0264-3707(02)00040-6.

Krabill, W., et al. (2004), Greenland Ice Sheet: Increased coastal thinning, *Geophys. Res. Lett.*, *31*, L24402, doi:10.1029/2004GL021533.

Marsh, P., and M. K. Woo (1984), Wetting front advance and freezing of meltwater within a snow cover: 1. Observations in the Canadian Arctic, *Water Resour. Res.*, *20*, 1853–1864, doi:10.1029/WR020i012p01853.

McConnell, J. R., E. Mosley-Thompson, D. H. Bromwich, R. C. Bales, and J. D. Kyne (2000), Interannual variations of snow accumulation on the Greenland Ice Sheet (1985–1996): New observations versus model predictions, *J. Geophys. Res.*, *105*, 4039–4046, doi:10.1029/1999JD901049.

Mernild, S. H., G. E. Liston, C. A. Hiemstra, and J. H. Christensen (2010), Greenland ice sheet surface mass-balance modeling in a 131-yr perspective, 1950–2080, *J. Hydrometeorol.*, *11*(1), 3–25, doi:10.1175/2009JHM1140.1.

Mote, T. L. (2007), Greenland surface melt trends 1973–2007: Evidence of a large increase in 2007, *Geophys. Res. Lett.*, *34*, L22507, doi:10.1029/2007GL031976.

Müller, F. (1962), Zonation in the accumulation area of the glaciers of Axel Heiberg Island, *J. Glaciol.*, *4*(33), 302–313.

Müller, F. (1976), On the thermal regime of a high-Arctic valley glacier, *J. Glaciol.*, *16*(74), 119–133.

Parizek, B. R., and R. B. Alley (2004), Implications of increased Greenland surface melt under global-warming scenarios: Ice-sheet simulations, *Quat. Sci. Rev.*, *23*(9–10), 1013–1027, doi:10.1016/j.quascirev.2003.12.024.

Parry, V., P. Nienow, D. Mair, J. Scott, B. Hubbard, K. Steffen, and D. Wingham (2007), Investigations of meltwater refreezing and density variations in the snowpack and firn within the percolation zone of the Greenland ice sheet, *Ann. Glaciol.*, *46*, 61–68, doi:10.3189/172756407782871332.

Paterson, W. S. B. (1981), *Physics of Glaciers*, 2nd ed., 380 pp., Pergamon, Oxford, U.K.

Pfeffer, W. T., and N. F. Humphrey (1996), Determination of timing and location of water movement and ice-layer formation by temperature measurements in sub-freezing snow, *J. Glaciol.*, *42*(141), 292–304.

Pfeffer, W. T., and N. F. Humphrey (1998), Formation of ice layers by infiltration and refreezing of meltwater, *Ann. Glaciol.*, *26*, 83–91.

Pfeffer, W. T., T. H. Illangasekare, and M. F. Meier (1990), Analysis and modeling of melt-water refreezing in dry snow, *J. Glaciol.*, *36*(123), 238–246.

Pfeffer, W. T., M. F. Meier, and T. H. Illangasekare (1991), Retention of Greenland runoff by refreezing: Implications for projected future sea-level change, *J. Geophys. Res.*, *96*, 22,117–22,124, doi:10.1029/91JC02502.

Rick, U. K., H. Rajaram, and W. T. Pfeffer (2008), Surface meltwater runoff and retention in the accumulation zone of the Greenland ice sheet, *Eos Trans. AGU*, *89*(53), Fall Meet. Suppl., Abstract C31B-0497.

Schwerdtfeger, P. (1963), The thermal properties of sea ice, *J. Glaciol.*, *4*(36), 789–807.

Shepherd, A., A. Hubbard, P. Nienow, M. King, M. McMillan, and I. Joughin (2009), Greenland ice sheet motion coupled with daily melting in late summer, *Geophys. Res. Lett.*, *36*, L01501, doi:10.1029/2008GL035758.

Steffen, K., J. E. Box, and W. Abdalati (1996), Greenland Climate Network, http://cires.colorado.edu/science/groups/steffen/gcnet/, U. S. Army Cold Reg. Res. and Eng. Lab., Hanover, N. H.

Steffen, K., S. V. Nghiem, R. Huff, and G. Neumann (2004), The melt anomaly of 2002 on the Greenland Ice Sheet from active and passive microwave satellite observations, *Geophys. Res. Lett.*, *31*, L20402, doi:10.1029/2004GL020444.

Sundal, A. V., A. Shepherd, P. Nienow, E. Hanna, S. Palmer, and P. Huybrechts (2011), Melt-induced speed-up of Greenland ice sheet offset by efficient subglacial drainage, *Nature*, *469*, 521–524, doi:10.1038/nature09740.

Tedesco, M. (2007), A new record in 2007 for melting in Greenland, *Eos Trans. AGU*, *88*(39), 383, doi:10.1029/2007EO390003.

van de Wal, R. S. W., W. Boot, M. R. van den Broeke, C. Smeets, C. H. Reijmer, J. J. A. Donker, and J. Oerlemans (2008), Large and rapid melt-induced velocity changes in the ablation zone of the Greenland Ice Sheet, *Science*, *321*(5885), 111–113, doi:10.1126/science.1158540.

Van Dusen, M. S. (1929), Thermal conductivity of non-metallic solids, in *International Critical Tables of Numerical Data, Physics, Chemistry and Technology*, edited by E. W. Washburn et al., pp. 216–217, McGraw-Hill, New York.

Zwally, H. J., W. Abdalati, T. Herring, K. Larson, J. Saba, and K. Steffen (2002), Surface melt-induced acceleration of Greenland ice-sheet flow, *Science*, *297*(5579), 218–222, doi:10.1126/science.1072708.

J. T. Harper, Department of Geosciences, University of Montana, 32 Campus Dr., #1296, Missoula, MT 59812, USA.

N. F. Humphrey, Department of Geology and Geophysics, University of Wyoming, 1000 E. University Ave., Laramie, WY 82071, USA. (neil@uwyo.edu)

W. T. Pfeffer, INSTAAR, University of Colorado at Boulder, 1560 30th St., Campus Box 450, Boulder, CO 80309, USA.